

Investigation of implicit time stepping for grid-induced stiffness in discontinuous Galerkin time-domain methods on unstructured triangular meshes

A. Catella¹ V. Dolean^{1,2} S. Lanteri¹

²University of Nice-Sophia Antipolis

J.A. Dieudonné Mathematics Laboratory, CNRS UMR 6621, 06108 Nice Cedex, France

¹INRIA, NACHOS project-team

2004 Route des Lucioles, BP 93, 06902 Sophia Antipolis Cedex, France

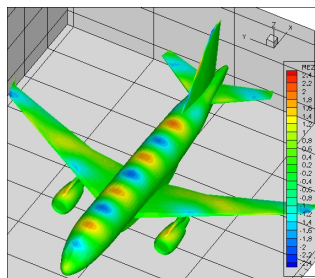
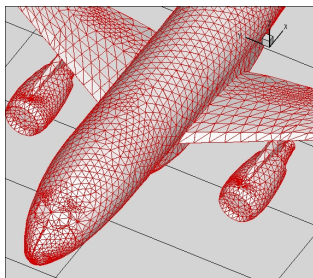
8th International Conference on Mathematical and
Numerical Aspects of Waves (Waves 2007)
23rd - 27th July 2007, University of Reading

- 1 Context and motivations
- 2 Implicit DGTD- \mathbb{P}_p method
- 3 Properties of the fully discrete scheme
- 4 Numerical results
- 5 Closure

- Time-domain electromagnetic wave propagation
- Irregularly shaped geometries, heterogeneous media
 - Unstructured, locally refined, triangular (2D)/tetrahedral (3D) meshes
- Numerical ingredients (starting point to this study)
 - Discontinuous Galerkin time-domain (DGTD) methods
 - Nodal (Lagrange type) polynomial interpolation
 - Explicit time integration

Context and motivations

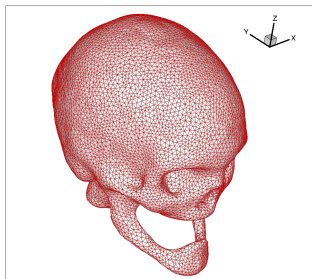
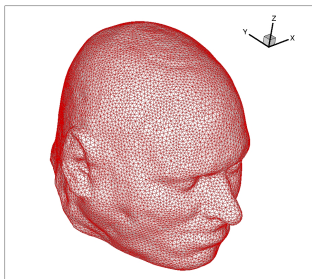
- Scattering of a plane wave by an aircraft, $F=1$ GHz
 - Mesh: # vertices = 153,821 , # tetrahedra = 883,374
 - $L_{\min} = 0.000601$ m , $L_{\max} = 0.121290$ m ($\approx \frac{\lambda}{2.5}$) , $L_{\text{avg}} = 0.039892$ m
 - $\Delta t_{\min} = 0.24$ picosec and $\Delta t_{\max} = 40.50$ picosec



Context and motivations

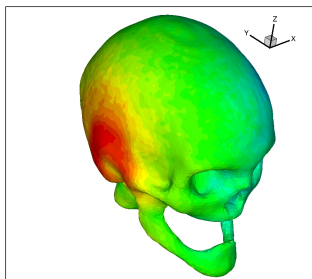
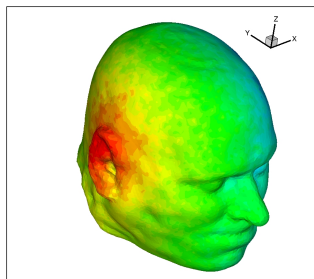
- Propagation in heterogeneous media, $F=1.8$ GHz
 - Mesh: # vertices = 311,259 , # tetrahedra = 1,862,136
 - $L_{\min} = 0.650$ mm , $L_{\max} = 8.055$ mm , $L_{\text{avg}} = 4.064$ mm
 - $\Delta t_{\min} = 0.019$ picosec and $\Delta t_{\max} = 0.203$ picosec

Tissue	L_{\min} (mm)	L_{\max} (mm)	L_{avg} (mm)	λ (mm)
Skin	1.339	8.055	4.070	26.73
Skull	1.613	7.786	4.069	42.25
CSF	0.650	7.232	4.059	20.33
Brain	0.650	7.993	4.009	25.26



Context and motivations

- Propagation in heterogeneous media, $F=1.8$ GHz
 - Mesh: # vertices = 311,259 , # tetrahedra = 1,862,136
 - $L_{\min} = 0.650$ mm , $L_{\max} = 8.055$ mm , $L_{\text{avg}} = 4.064$ mm
 - $\Delta t_{\min} = 0.019$ picosec and $\Delta t_{\max} = 0.203$ picosec



- Possible routes to overcome grid-induced stiffness
 - Local time-step strategies with explicit time integration
 - Locally implicit (hybrid explicit/implicit) time integration
- Objective of this study
 - Investigate strengthes and weaknesses of implicit time integration
 - Numerical aspects (stability, dispersion error)
 - Computational aspects

Context and motivations

Discontinuous Galerkin methods: some generalities

- Initially introduced to solve neutron transport problems (W. Reed and T. Hill, 1973)
- Became popular as a framework for solving hyperbolic or mixed hyperbolic/parabolic problems
- Recently developed for elliptic problems
- Somewhere between a finite element and a finite volume method, gathering many good features of both
- Main properties
 - Can easily deal with discontinuous coefficients and solutions
 - Can handle unstructured, non-conforming meshes
 - Yield local finite element mass matrices
 - High-order accurate methods with compact stencils
 - Naturally lead to discretization and interpolation order adaptivity
 - Amenable to efficient parallelization

Context and motivations

Discontinuous Galerkin methods: related works for time-domain Maxwell's equations

- F. Bourdel, P.A. Mazet and P. Helluy
Proc. 10th Inter. Conf. on Comp. Meth. in Appl. Sc. and Eng., 1992
 - Triangular meshes, first-order upwind DG method (i.e FV method)
 - Time-domain and time-harmonic Maxwell equations
- M. Remaki and L. Fezoui, INRIA RR-3501, 1998
 - Time-domain Maxwell equations
 - Triangular meshes, P1 interpolation, Runge-Kutta time integration (RKDG)
- J.S. Hesthaven and T. Warburton (J. Comput. Phys., Vol. 181, 2002)
 - Tetrahedral meshes, high order Lagrange polynomials, upwind flux
 - Runge-Kutta time integration
- B. Cockburn, F. Li and C.-W. Shu (J. Comput. Phys., Vol. 194, 2004)
 - Locally divergence-free RKDG formulation
- L. Fezoui, S. Lanteri, S. Lohrengel and S. Piperno (M2AN, Vol. 39, No. 6, 2005)
 - Tetrahedral meshes, high order Lagrange polynomials
 - Leap-frog time integration scheme, centered flux
- G. Cohen, X. Ferrieres and S. Pernet (J. Comput. Phys., Vol. 217, 2006)
 - Hexahedral meshes, high order Lagrange polynomials, penalized formulation
 - Leap-frog time integration scheme

- 1 Context and motivations
- 2 Implicit DGTD- \mathbb{P}_p method
- 3 Properties of the fully discrete scheme
- 4 Numerical results
- 5 Closure

- 1 Context and motivations
- 2 Implicit DGTD- \mathbb{P}_p method**
- 3 Properties of the fully discrete scheme
- 4 Numerical results
- 5 Closure

- Time-domain Maxwell's equations

$$\begin{cases} \varepsilon \partial_t \mathbf{E} - \text{curl}(\mathbf{H}) = 0 \\ \mu \partial_t \mathbf{H} + \text{curl}(\mathbf{E}) = 0 \end{cases}$$

$$\mathbf{E} = (E_x, E_y, E_z)^t \quad \text{and} \quad \mathbf{H} = (H_x, H_y, H_z)^t$$

- Boundary conditions: $\partial\Omega = \Gamma_a \cup \Gamma_m$

$$\begin{cases} \mathbf{n} \times \mathbf{E} = 0 \text{ on } \Gamma_m \\ \mathbf{n} \times \mathbf{E} - \sqrt{\frac{\mu}{\varepsilon}} \mathbf{n} \times (\mathbf{H} \times \mathbf{n}) = \mathbf{n} \times \mathbf{E}_{\text{inc}} - \sqrt{\frac{\mu}{\varepsilon}} \mathbf{n} \times (\mathbf{H}_{\text{inc}} \times \mathbf{n}) \text{ on } \Gamma_a \end{cases}$$

- System formulation: $\mathbf{W} = (\mathbf{E}, \mathbf{H})^t$

$$\begin{cases} G_0 \partial_t \mathbf{W} + G_x \partial_x \mathbf{W} + G_y \partial_y \mathbf{W} + G_z \partial_z \mathbf{W} = 0 \text{ in } \Omega \\ (M_{\Gamma_m} - G_n) \mathbf{W} = 0 \text{ on } \Gamma_m \\ (M_{\Gamma_a} - G_n) \mathbf{W} = (M_{\Gamma_a} - G_n) \mathbf{W}_{\text{inc}} \text{ on } \Gamma_a \end{cases}$$

- Flux matrices

- $G_l \mathbf{W} = (\mathbf{H} \times \mathbf{e}_l, -\mathbf{E} \times \mathbf{e}_l)^t$, $\{\mathbf{e}_l\}_{x,y,z}$ is the canonical base of \mathbb{R}^3
- $G_n \mathbf{W} = (\mathbf{H} \times \mathbf{n}, -\mathbf{E} \times \mathbf{n})^t$

$$G_0 = \begin{pmatrix} \varepsilon \text{Id}_3 & 0_{3 \times 3} \\ 0_{3 \times 3} & \mu \text{Id}_3 \end{pmatrix}$$

$$G_n = \begin{pmatrix} 0_{3 \times 3} & N_n \\ N_n^t & 0_{3 \times 3} \end{pmatrix} \text{ with } N_n = \begin{pmatrix} 0 & \mathbf{n}_z & -\mathbf{n}_y \\ -\mathbf{n}_z & 0 & \mathbf{n}_x \\ \mathbf{n}_y & -\mathbf{n}_x & 0 \end{pmatrix}$$

- Diagonalization: $G_{\mathbf{n}} = T\Lambda T^{-1}$ and $G_{\mathbf{n}}^{\pm} = T\Lambda^{\pm}T^{-1}$
- Boundary flux matrices

$$\begin{cases} M_{\Gamma_m} = \begin{pmatrix} 0_{3 \times 3} & N_{\mathbf{n}} \\ -N_{\mathbf{n}}^t & 0_{3 \times 3} \end{pmatrix} \\ M_{\Gamma_a} = |G_{\mathbf{n}}| \end{cases}$$

- First-order absorbing condition: $(M_{\Gamma_a} - G_{\mathbf{n}})\mathbf{W} = 0 \Leftrightarrow G_{\mathbf{n}}^{-}\mathbf{W} = 0$

Implicit DGTD- \mathbb{P}_p method

- Semi-discretization in time
 - Crank-Nicolson scheme
 - \mathbf{W}^n : approximation of \mathbf{W} at time $t_n = n\Delta t$

$$G_0 \left(\frac{\mathbf{W}^{n+1} - \mathbf{W}^n}{\Delta t} \right) + (G_x \partial_x + G_y \partial_y + G_z \partial_z) \left(\frac{\mathbf{W}^{n+1} + \mathbf{W}^n}{2} \right) = 0$$

- Boundary value problem: for each t_n ,

$$\begin{cases} \beta G_0 \mathbf{W} + (G_x \partial_x + G_y \partial_y + G_z \partial_z) \mathbf{W} = \mathbf{F} & \text{in } \Omega \\ (M_{\Gamma_m} - G_n) \mathbf{W} = 0 & \text{on } \Gamma_m \\ (M_{\Gamma_a} - G_n) \mathbf{W} = (M_{\Gamma_a} - G_n) \mathbf{W}_{\text{inc}} & \text{on } \Gamma_a \end{cases}$$

- $\beta = \frac{2}{\Delta t}$ and $\mathbf{W} = \mathbf{W}^{n+1}$
- $\mathbf{F} = \beta G_0 \mathbf{W}^n - (G_x \partial_x + G_y \partial_y + G_z \partial_z) \mathbf{W}^n$

- Semi-discrete electromagnetic energy

$$\text{Let } \mathcal{E}^n = \frac{1}{2} \int_{\Omega} (\mathbf{W}^n)^t (G_0 \mathbf{W}^n) dx = \frac{1}{2} \int_{\Omega} \varepsilon \|\mathbf{E}^n\|^2 dx + \frac{1}{2} \int_{\Omega} \mu \|\mathbf{H}^n\|^2 dx$$

Then \mathcal{E}^n is exactly conserved if $\Gamma_a = \emptyset$ or $\mathcal{E}^{n+1} \leq \mathcal{E}^n$ if $\Gamma_a \neq \emptyset$

$$\frac{\mathcal{E}^{n+1} - \mathcal{E}^n}{\Delta t} = - \int_{\Omega} \left(\frac{\mathbf{W}^{n+1} + \mathbf{W}^n}{2} \right)^t \mathcal{G}_{xyz} \left(\frac{\mathbf{W}^{n+1} + \mathbf{W}^n}{2} \right) dx$$

with $\mathcal{G}_{xyz} \equiv (G_x \partial_x + G_y \partial_y + G_z \partial_z)$ and,

$$\int_{\Omega} \mathbf{W}^t \mathcal{G}_{xyz} \mathbf{W} = \frac{1}{2} \int_{\Gamma_m} \mathbf{W}^t (M_{\Gamma_m} \mathbf{W}) ds + \frac{1}{2} \int_{\Gamma_a} \mathbf{W}^t (M_{\Gamma_a} \mathbf{W}) ds$$

but M_{Γ_m} skew-symmetric and $|G_n|$ positive then,

$$\int_{\Omega} \mathbf{W}^t \mathcal{G}_{xyz} \mathbf{W} = \frac{1}{2} \int_{\Gamma_a} \mathbf{W}^t (|G_n| \mathbf{W}) ds \geq 0$$

- Discretization in space

- Triangulation of Ω : $\overline{\Omega}_h \equiv \mathcal{T}_h = \bigcup_{K \in \mathcal{T}_h} \overline{K}$
 - \mathcal{F}_0 : set of purely internal faces
 - \mathcal{F}_m and \mathcal{F}_a : sets of faces on the boundaries Γ_m and Γ_a
- $V_h = \{ \mathbf{V} \in [L^2(\Omega)]^3 \times [L^2(\Omega)]^3 \mid \forall K \in \mathcal{T}_h, \mathbf{V}|_K \in \mathbb{P}_p(K) \}$
- Variational formulation

$$\int_K (G_0 \partial_t \mathbf{W}_h)^t \mathbf{V} dx - \int_K \mathbf{W}_h^t \left(\sum_{l \in \{x,y,z\}} G_l \partial_l \mathbf{V} \right) dx + \sum_{F \in \partial K} \int_F (\Phi_F(\mathbf{W}_h))^t \mathbf{V} ds = 0, \quad \forall \mathbf{V} \in V_h$$

- Numerical flux

$$\Phi_F(\mathbf{W}_h) = \begin{cases} I_{F,K} G_{n_F} \{ \mathbf{W}_h \} & \text{if } F \in \mathcal{F}_0 \\ \frac{1}{2} (M_{F,K} + I_{F,K} G_{n_F}) \mathbf{W}_h & \text{if } F \in (\mathcal{F}_m \cup \mathcal{F}_a) \end{cases}$$

- Discretization in space

- Boundary flux matrices: $M_{F,K} = \begin{cases} I_{F,K} \begin{pmatrix} 0_{3 \times 3} & N_{\mathbf{n}_F} \\ -N_{\mathbf{n}_F}^t & 0_{3 \times 3} \end{pmatrix} & \text{if } F \in \mathcal{F}_m \\ |G_{\mathbf{n}_F}| & \text{if } F \in \mathcal{F}_a \end{cases}$

- For $F = K \cap \tilde{K}$ (\tilde{K} neighbor of K): $\begin{cases} \llbracket \mathbf{V}_h \rrbracket_F = I_{F,K} \mathbf{V}_{h|K} + I_{F,\tilde{K}} \mathbf{V}_{h|\tilde{K}} \\ \{\mathbf{V}_h\}_F = \frac{1}{2}(\mathbf{V}_{h|K} + \mathbf{V}_{h|\tilde{K}}) \end{cases}$

$$\begin{aligned} \int_{\Omega_h} (G_0 \partial_t \mathbf{W}_h)^t \mathbf{V} dx - \sum_{K \in \mathcal{T}_h} \int_K \mathbf{W}_h^t \left(\sum_{l \in \{x,y,z\}} G_l \partial_l \mathbf{V} \right) dx \\ + \sum_{F \in \mathcal{F}_m \cup \mathcal{F}_a} \int_F \left(\frac{1}{2} (M_{F,K} + I_{F,K} G_{\mathbf{n}_F}) \mathbf{W}_h \right)^t \mathbf{V} ds \\ + \sum_{F \in \mathcal{F}_0} \int_F (G_{\mathbf{n}_F} \{\mathbf{W}_h\}_F)^t \llbracket \mathbf{V} \rrbracket_F ds = 0 \end{aligned}$$

- 1 Context and motivations
- 2 Implicit DGTD- \mathbb{P}_p method
- 3 Properties of the fully discrete scheme**
- 4 Numerical results
- 5 Closure

Properties of the fully discrete scheme

- Equivalent, face oriented, formulation

Since (with \tilde{K} a neighboring element of K),

$$\begin{aligned} \sum_{F \in \mathcal{F}_0} \int_F (\mathbf{G}_{n_F} \{\mathbf{W}_h\}_F)^t \llbracket \mathbf{V} \rrbracket_F ds &= \sum_{K \in \mathcal{T}_h} \sum_{\substack{F \in \partial K \\ F \in \mathcal{F}_0}} \int_F \frac{1}{2} (\mathbf{G}_{n_F} \mathbf{W}_{h|K})^t (I_{F,K} \mathbf{V}|_K) ds \\ &+ \sum_{K \in \mathcal{T}_h} \sum_{\substack{F \in \partial K \\ F \in \mathcal{F}_0}} \int_F \frac{1}{2} (\mathbf{G}_{n_F} \mathbf{W}_{h|\tilde{K}})^t (I_{F,K} \mathbf{V}|_K) ds \end{aligned}$$

Then,

$$\begin{aligned} &2 \int_{\Omega_h} (G_0 \partial_t \mathbf{W}_h)^t \mathbf{V} dx - \sum_{K \in \mathcal{T}_h} \int_K \mathbf{W}_h^t \left(\sum_{I \in \{x,y,z\}} G_I \partial_I \mathbf{V} \right) dx + \\ &\sum_{K \in \mathcal{T}_h} \int_K \left(\sum_{I \in \{x,y,z\}} G_I \partial_I \mathbf{W}_h \right)^t \mathbf{V} dx + \sum_{F \in \mathcal{F}_m \cup \mathcal{F}_a} \int_F (M_{F,K} \mathbf{W}_h)^t \mathbf{V} ds + \\ &\sum_{F \in \mathcal{F}_0} \int_F \left[(\mathbf{G}_{n_F} \mathbf{W}_{h|K})^t (I_{F,\tilde{K}} \mathbf{V}|\tilde{K}) + (\mathbf{G}_{n_F} \mathbf{W}_{h|\tilde{K}})^t (I_{F,K} \mathbf{V}|K) \right] ds = 0 \end{aligned}$$

Properties of the fully discrete scheme

- Bilinear forms

Find $\mathbf{W}_h \in V_h$ such that $\forall \mathbf{V} \in V_h$

$$a(\partial_t \mathbf{W}, \mathbf{V}) + b(\mathbf{W}, \mathbf{V}) + c(\mathbf{W}, \mathbf{V}) = 0, \forall \mathbf{V} \in V_h$$

$$\left\{ \begin{array}{l} a(\mathbf{W}, \mathbf{V}) = 2 \int_{\Omega_h} (G_0 \mathbf{W})^t \mathbf{V} dx \\ b(\mathbf{W}, \mathbf{V}) = - \int_{\Omega_h} \mathbf{W}^t \left(\sum_{I \in \{x,y,z\}} G_I \partial_I \mathbf{V} \right) dx + \int_{\Omega_h} \left(\sum_{I \in \{x,y,z\}} G_I \partial_I \mathbf{W} \right)^t \mathbf{V} dx \\ c(\mathbf{W}, \mathbf{V}) = \sum_{F \in \mathcal{F}_0} \int_F \left[(G_{n_F} \mathbf{W}|_K)^t (I_{F,\tilde{K}} \mathbf{V}|_{\tilde{K}}) + (G_{n_F} \mathbf{W}|_{\tilde{K}})^t (I_{F,K} \mathbf{V}|_K) \right] ds \\ \quad + \sum_{F \in \mathcal{F}_m \cup \mathcal{F}_a} \int_F (M_{F,K} \mathbf{W})^t \mathbf{V} ds \end{array} \right.$$

Properties of the fully discrete scheme

- Properties of the bilinear forms
 - $b(\mathbf{W}, \mathbf{V})$ is skew-symmetric
 - Since G_{n_F} is symmetric and $I_{F,\tilde{K}} = -I_{F,K}$ then,

$$c(\mathbf{W}_h, \mathbf{W}_h) = \sum_{F \in \mathcal{F}_m \cup \mathcal{F}_a} \int_F (M_{F,K} \mathbf{W}_h)^t \mathbf{W}_h ds$$

but M_{Γ_m} is skew-symmetric thus,

$$c(\mathbf{W}_h, \mathbf{W}_h) = \sum_{F \in \mathcal{F}_a} \int_F (|G_{n_F}| \mathbf{W}_h)^t \mathbf{W}_h ds$$

- Fully discrete formulation based on Crank-Nicolson scheme

Find $\mathbf{W}_h^{n+1} \in V_h$ such that $\forall \mathbf{V} \in V_h$

$$\begin{aligned} \beta a(\mathbf{W}_h^{n+1}, \mathbf{V}) + b(\mathbf{W}_h^{n+1}, \mathbf{V}) + c(\mathbf{W}_h^{n+1}, \mathbf{V}) \\ = \beta a(\mathbf{W}_h^n, \mathbf{V}) - b(\mathbf{W}_h^n, \mathbf{V}) - c(\mathbf{W}_h^n, \mathbf{V}) \end{aligned}$$

with $\beta = \frac{2}{\Delta t}$

Properties of the fully discrete scheme

- Well-posedness of the discrete problem

The homogeneous discrete problem,

$$\text{Find } \mathbf{W}_h \in V_h \text{ such that} \\ \beta a(\mathbf{W}_h, \mathbf{V}) + b(\mathbf{W}_h, \mathbf{V}) + c(\mathbf{W}_h, \mathbf{V}) = 0, \forall \mathbf{V} \in V_h$$

possesses only the trivial solution

- Elements of the proof
 - $b(\mathbf{W}, \mathbf{V})$ is skew-symmetric
 - G_0 is symmetric positive definite
 - $|G_{n_F}|$ is positive

$$\begin{aligned} \beta a(\mathbf{W}_h, \mathbf{W}_h) + b(\mathbf{W}_h, \mathbf{W}_h) \\ + c(\mathbf{W}_h, \mathbf{W}_h) &= 2\beta \int_{\Omega_h} (G_0 \mathbf{W}_h)^t \mathbf{W}_h dx \\ &+ \sum_{F \in \mathcal{F}_a} \int_F \mathbf{W}_h^t |G_{n_F}| \mathbf{W}_h ds = 0 \end{aligned}$$

Properties of the fully discrete scheme

- Fully discrete energy: $\mathcal{E}_h^n = \frac{1}{4}a(\mathbf{W}_h^n, \mathbf{W}_h^n)$

Then \mathcal{E}^n is exactly conserved if $\Gamma_a = \emptyset$ or $\mathcal{E}_h^{n+1} \leq \mathcal{E}_h^n$ if $\Gamma_a \neq \emptyset$

- Elements of the proof

- Choose as a test function $\mathbf{V} = \frac{\mathbf{W}_h^{n+1} + \mathbf{W}_h^n}{2}$
- $b(\mathbf{W}, \mathbf{V})$ is a skew-symmetric
- G_{n_F} and $|G_{n_F}|$ are symmetric

- Convergence of the fully discrete scheme

- L. Fezoui, S. Lanteri, S. Lohrengel and S. Piperno
M2AN, Vol. 39, No. 6, 2005

$$\mathcal{O}(Th^{\min(s,p)}) + \mathcal{O}(\Delta t^2)$$

for the total error in $C^0([0, T]; L^2(\Omega))$ with $s > \frac{1}{2}$ a regularity parameter

Properties of the fully discrete scheme

- Fully discrete energy: $\mathcal{E}_h^n = \frac{1}{4}a(\mathbf{W}_h^n, \mathbf{W}_h^n)$

Then \mathcal{E}^n is exactly conserved if $\Gamma_a = \emptyset$ or $\mathcal{E}_h^{n+1} \leq \mathcal{E}_h^n$ if $\Gamma_a \neq \emptyset$

- Elements of the proof

- Choose as a test function $\mathbf{V} = \frac{\mathbf{W}_h^{n+1} + \mathbf{W}_h^n}{2}$
- $b(\mathbf{W}, \mathbf{V})$ is a skew-symmetric
- G_{n_F} and $|G_{n_F}|$ are symmetric

- Convergence of the fully discrete scheme

- L. Fezoui, S. Lanteri, S. Lohrengel and S. Piperno
M2AN, Vol. 39, No. 6, 2005

$$\mathcal{O}(Th^{\min(s,p)}) + \mathcal{O}(\Delta t^2)$$

for the total error in $C^0([0, T]; L^2(\Omega))$ with $s > \frac{1}{2}$ a regularity parameter

- 1 Context and motivations
- 2 Implicit DGTD- \mathbb{P}_p method
- 3 Properties of the fully discrete scheme
- 4 Numerical results**
- 5 Closure

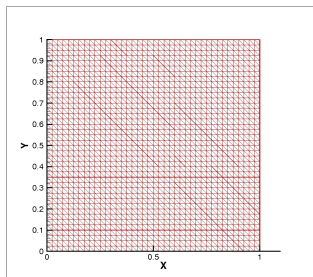
- Two-dimensional Maxwell's equation (TM)

$$\begin{cases} \mu \frac{\partial H_x}{\partial t} + \frac{\partial E_z}{\partial y} = 0 \\ \mu \frac{\partial H_y}{\partial t} - \frac{\partial E_z}{\partial x} = 0 \\ \varepsilon \frac{\partial E_z}{\partial t} - \frac{\partial H_y}{\partial x} + \frac{\partial H_x}{\partial y} = 0 \end{cases}$$

- Implicit DGTD- \mathbb{P}_p method
 - Triangular mesh
 - Sparse block matrix, $3n_p \times 3n_p$ (with $n_p = ((p+1)(p+2))/2$)
 - MUMPS multifrontal sparse matrix solver
(P.R. Amestoy, I.S. Duff and J.-Y. L'Excellent, CMAME, Vol. 184, 2000)
 - LU factors computed before entering the time stepping loop

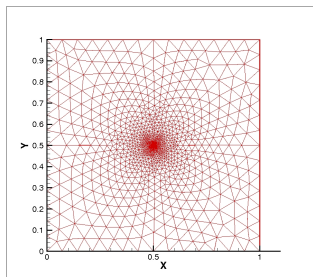
Numerical results

Eigenmode in a metallic cavity



vertices = 1,681
elements = 3,200

$(\Delta t)_u = 58.92$ picosec

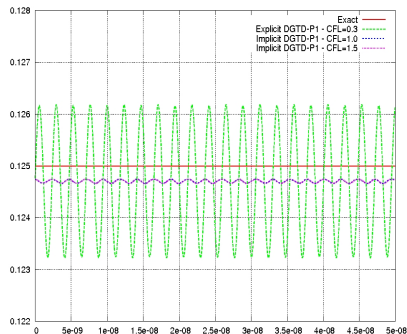
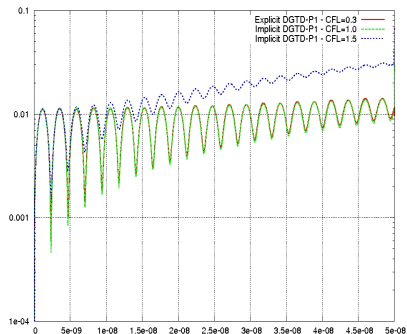


vertices = 1,400
elements = 2,742

$(\Delta t)_m = 1.44$ picosec
 $(\Delta t)_M = 235.54$ picosec

Numerical results

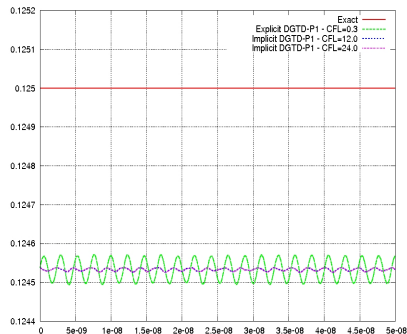
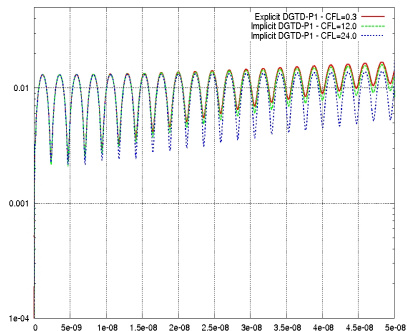
Eigenmode in a metallic cavity



DGTD- \mathbb{P}_1 method: time evolutions of the L2 error (left) and discrete energy (right)
Uniform mesh

Numerical results

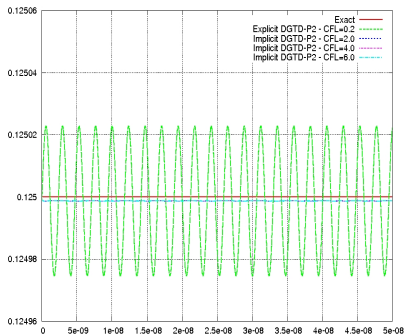
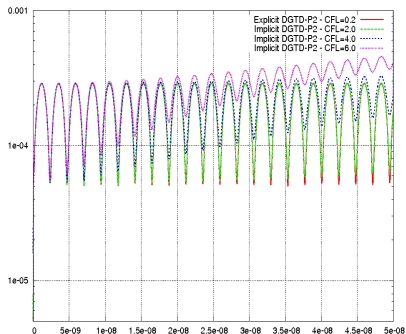
Eigenmode in a metallic cavity



DGTD- \mathbb{P}_1 method: time evolutions of the L2 error (left) and discrete energy (right)
Non-uniform mesh

Numerical results

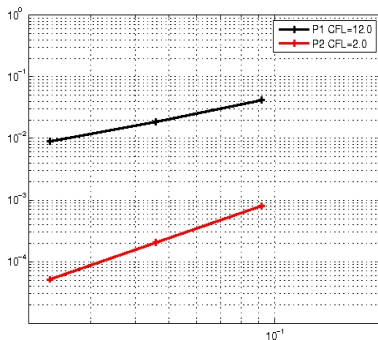
Eigenmode in a metallic cavity



DGTD- \mathbb{P}_2 method: time evolutions of the L2 error (left) and discrete energy (right)
Non-uniform mesh

Numerical results

Eigenmode in a metallic cavity



Numerical convergence of the implicit DGTD- \mathbb{P}_1 and DGTD- \mathbb{P}_2 methods
Non-uniform mesh

Global (space and time) L2 error versus maximal edge length (logarithmic scales)

Slopes: 1.11 (DGTD- \mathbb{P}_1 method) and 1.98 (DGTD- \mathbb{P}_2 method)

Numerical results

Eigenmode in a metallic cavity

Computing times (AMD Opteron 2 GHz based workstation)

Time integration	Method	CFL- \mathbb{P}_p	CPU time
Explicit	DGTD- \mathbb{P}_1	0.3	15 sec
Implicit	-	1.0	44 sec
-	-	1.5	30 sec

Uniform mesh

Time integration	Method	CFL- \mathbb{P}_p	CPU time
Explicit	DGTD- \mathbb{P}_1	0.3	443 sec
Implicit	-	12.0	133 sec
-	-	24.0	67 sec
Explicit	DGTD- \mathbb{P}_2	0.2	2057 sec
Implicit	-	2.0	1923 sec
-	-	4.0	938 sec
-	-	6.0	620 sec

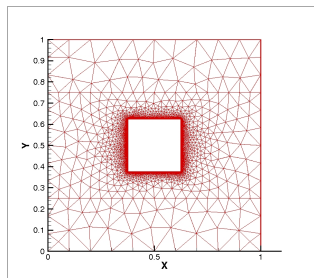
Non-uniform mesh

Factorization: CPU time, RAM size (LU/total)

< 1 sec, 13 MB/26 MB (DGTD- \mathbb{P}_1) and 2 sec, 34 MB/64 MB (DGTD- \mathbb{P}_2)

Numerical results

Scattering of a plane wave by a PEC square

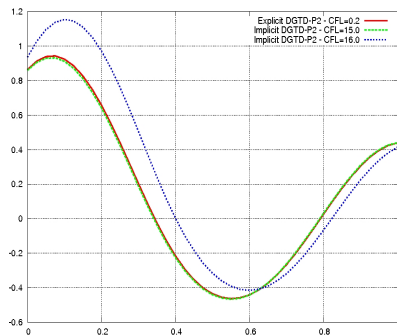
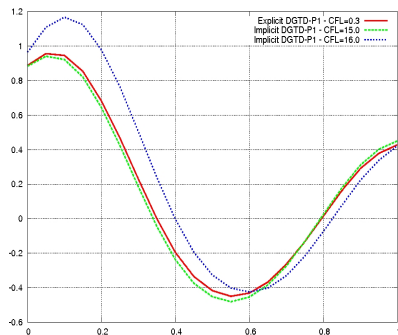


vertices = 6,018
elements = 10,792

$(\Delta t)_m = 0.95$ picosec
 $(\Delta t)_M = 328.60$ picosec

Numerical results

Scattering of a plane wave by a PEC square

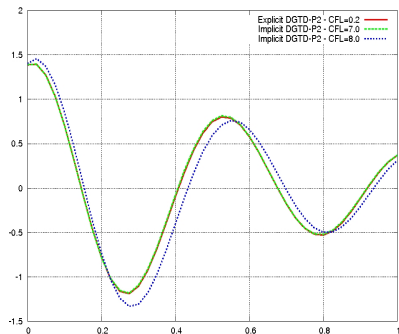
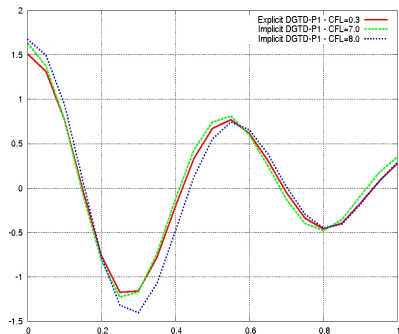


F=300 MHz: 1D distribution of $DFT(E_z)$, $y = 0.75$ m

Left: DGTD- \mathbb{P}_1 method - Right: DGTD- \mathbb{P}_2 method

Numerical results

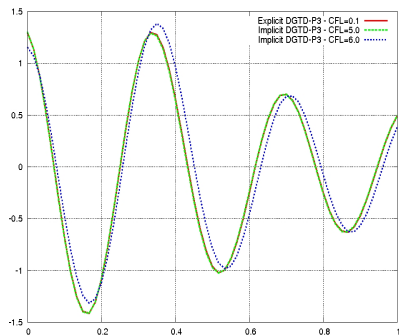
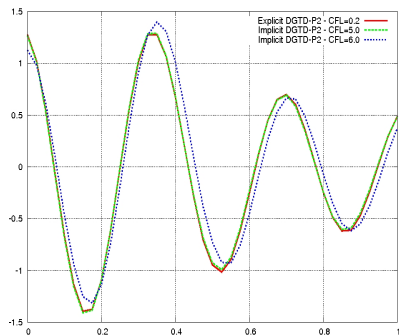
Scattering of a plane wave by a PEC square



F=600 MHz: 1D distribution of $DFT(E_z)$, $y = 0.75$ m
Left: DGTD- \mathbb{P}_1 method - Right: DGTD- \mathbb{P}_2 method

Numerical results

Scattering of a plane wave by a PEC square



F=900 MHz: 1D distribution of $DFT(E_z)$, $y = 0.75$ m

Left: DGTD- \mathbb{P}_2 method - Right: DGTD- \mathbb{P}_3 method

Numerical results

Scattering of a plane wave by a PEC square

Computing times (AMD Opteron 2 GHz based workstation)

Frequency	Time integration	Method	CFL- \mathbb{P}_p	CPU time
300 MHz	Explicit	DGTD- \mathbb{P}_1	0.3	1602 sec
-	Implicit	-	15.0	370 sec
-	Explicit	DGTD- \mathbb{P}_2	0.2	5677 sec
-	Implicit	-	15.0	762 sec
600 MHz	Explicit	DGTD- \mathbb{P}_1	0.3	758 sec
-	Implicit	-	7.0	383 sec
-	Explicit	DGTD- \mathbb{P}_2	0.2	3074 sec
-	Implicit	-	7.0	767 sec
900 MHz	Explicit	DGTD- \mathbb{P}_2	0.2	2191 sec
-	Implicit	-	5.0	746 sec
-	Explicit	DGTD- \mathbb{P}_3	0.1	8771 sec
-	Implicit	-	5.0	1591 sec

Numerical results

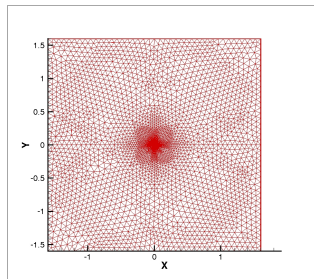
Scattering of a plane wave by a PEC square

Computing times (AMD Opteron 2 GHz based workstation)
Factorization phase

Frequency	Method	CFL- \mathbb{P}_p	CPU time	RAM size (LU/total)
300 MHz	DGTD- \mathbb{P}_1	15.0	3 sec	38 MB/ 73 MB
-	DGTD- \mathbb{P}_2	15.0	8 sec	106 MB/194 MB
600 MHz	DGTD- \mathbb{P}_1	7.0	3 sec	38 MB/ 73 MB
-	DGTD- \mathbb{P}_2	7.0	8 sec	106 MB/194 MB
900 MHz	DGTD- \mathbb{P}_2	5.0	8 sec	106 MB/194 MB
-	DGTD- \mathbb{P}_3	5.0	16 sec	229 MB/425 MB

Numerical results

Scattering of a plane wave by a dielectric cylinder



vertices = 4,108

elements = 8,054

Cylinder: $R=0.6$ m

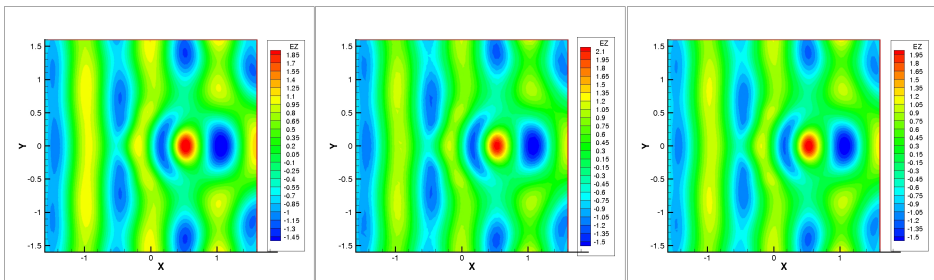
$F=300$ MHz, $\varepsilon_{r,1} = 1.0$ and $\varepsilon_{r,2} = 2.25$

$(\Delta t)_m = 2.09$ picosec

$(\Delta t)_M = 309.63$ picosec

Numerical results

Scattering of a plane wave by a dielectric cylinder



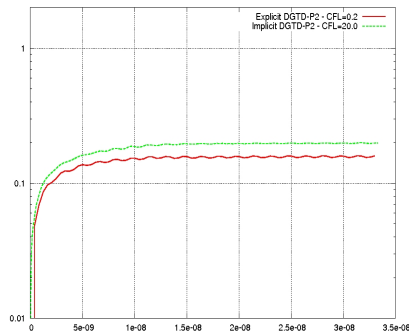
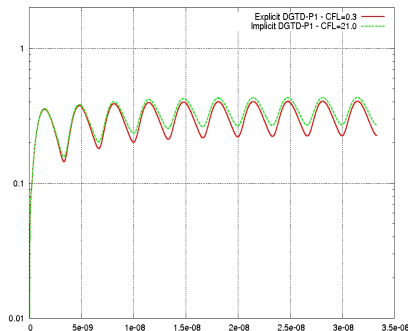
F=300 MHz: contour lines of E_z after 10 periods

Left: exact solution

Middle: implicit DGTD- \mathbb{P}_1 method - Right: implicit DGTD- \mathbb{P}_2 method

Numerical results

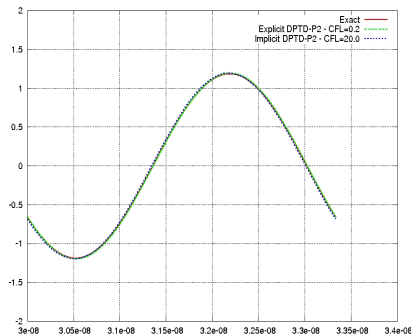
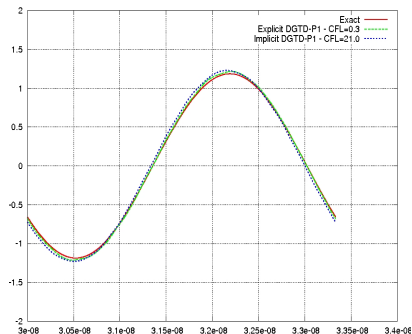
Scattering of a plane wave by a dielectric cylinder



F=300 MHz: time evolution of the L2 error
Left: DGTD- \mathbb{P}_1 method - Right: DGTD- \mathbb{P}_2 method

Numerical results

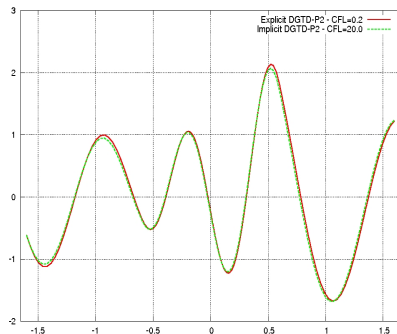
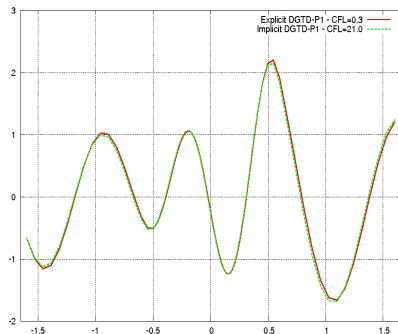
Scattering of a plane wave by a dielectric cylinder



F=300 MHz: time evolution of E_z (zoom on the last of 10 periods)
Left: DGTD- \mathbb{P}_1 method - Right: DGTD- \mathbb{P}_2 method

Numerical results

Scattering of a plane wave by a dielectric cylinder



F=300 MHz: 1D distribution of $DFT(E_z)$, $y = 0.0$ m
Left: DGTD- \mathbb{P}_1 method - Right: DGTD- \mathbb{P}_2 method

Numerical results

Scattering of a plane wave by a dielectric cylinder

Computing times (AMD Opteron 2 GHz based workstation)

Time integration	Method	CFL- \mathbb{P}_p	CPU time
Explicit	DGTD- \mathbb{P}_1	0.3	542 sec
Implicit	-	21.0	102 sec
Explicit	DGTD- \mathbb{P}_2	0.2	1892 sec
Implicit	DGTD- \mathbb{P}_2	20.0	218 sec

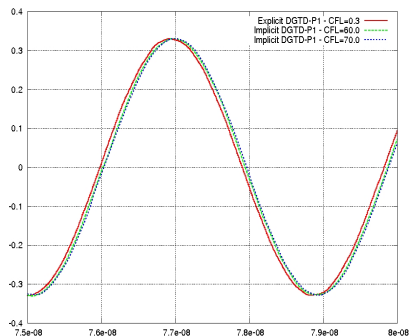
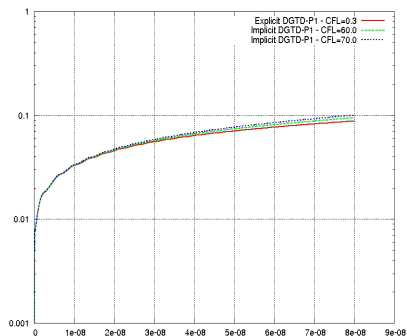
Factorization phase

Method	CFL- \mathbb{P}_p	CPU time	RAM size (LU/total)
DGTD- \mathbb{P}_1	20.0	3 sec	40 MB/ 70 MB
DGTD- \mathbb{P}_2	20.0	6 sec	107 MB/181 MB

Numerical results

Preliminary result in 3D: eigenmode in a metallic cavity

- $\#$ vertices = 3,815 and $\#$ tetrahedra = 19,540
- $(\Delta t)_m = 0.84$ picosec and $(\Delta t)_M = 107.10$ picosec



DGTD- \mathbb{P}_1 method: time evolutions of the L2 error (left) and of E_z (right)

Numerical results

Preliminary result in 3D: eigenmode in a metallic cavity

Computing times (AMD Opteron 2.2 GHz cluster with Myrinet)
Simulation for a duration of 80 nanosec, 8 processors

Time integration	Method	CFL- \mathbb{P}_p	CPU time
Explicit	DGTD- \mathbb{P}_1	0.3	2670 sec
Implicit	-	60.0	1312 sec
-	-	70.0	1049 sec

Factorization phase

CFL	CPU time	LU RAM size (min/max)	Total RAM size (mn/max)
60.0	1484 sec	343 MB/600 MB	1061 MB/1608 MB
70.0	1052 sec	-	-

- 1 Context and motivations
- 2 Implicit DGTD- \mathbb{P}_p method
- 3 Properties of the fully discrete scheme
- 4 Numerical results
- 5 Closure

- Implicit DGTD- \mathbb{P}_p method
 - Second order accurate in time and $p + 1$ -th order accurate in space
 - Non-dissipative and unconditionally stable
 - Allowable CFL (global time step) is dictated by physical considerations
- Performance issues
 - LU factorization is a viable option in 2D
 - For a fixed p , CPU explicit/CPU implicit \searrow when frequency $F \nearrow$
 - For a fixed F , CPU explicit/CPU implicit \nearrow when interpolation order $p \nearrow$
- Future works
 - Extension to the 3D case
 - Locally implicit DGTD- \mathbb{P}_p method
 - Domain decomposition for a hybrid iterative/direct linear solver
 - Analytical dispersion analysis
 - High order time integration methods

Thank you for your attention!

- Implicit DGTD- \mathbb{P}_p method
 - Second order accurate in time and $p + 1$ -th order accurate in space
 - Non-dissipative and unconditionally stable
 - Allowable CFL (global time step) is dictated by physical considerations
- Performance issues
 - LU factorization is a viable option in 2D
 - For a fixed p , CPU explicit/CPU implicit \searrow when frequency $F \nearrow$
 - For a fixed F , CPU explicit/CPU implicit \nearrow when interpolation order $p \nearrow$
- Future works
 - Extension to the 3D case
 - Locally implicit DGTD- \mathbb{P}_p method
 - Domain decomposition for a hybrid iterative/direct linear solver
 - Analytical dispersion analysis
 - High order time integration methods

Thank you for your attention!

- Implicit DGTD- \mathbb{P}_p method
 - Second order accurate in time and $p + 1$ -th order accurate in space
 - Non-dissipative and unconditionally stable
 - Allowable CFL (global time step) is dictated by physical considerations
- Performance issues
 - LU factorization is a viable option in 2D
 - For a fixed p , CPU explicit/CPU implicit \searrow when frequency $F \nearrow$
 - For a fixed F , CPU explicit/CPU implicit \nearrow when interpolation order $p \nearrow$
- Future works
 - Extension to the 3D case
 - Locally implicit DGTD- \mathbb{P}_p method
 - Domain decomposition for a hybrid iterative/direct linear solver
 - Analytical dispersion analysis
 - High order time integration methods

Thank you for your attention!